

An Improved and Fast Approach to Parameter Estimation of SFM Signal Using Carson's Rule

XUEJUN SUN, BIN TANG

School of Electronic Engineering

University of Electronic Science and Technology of China

No. 2006, Xi Yuan Road, Hi-Tech Zone (West), Chengdu

P.R. CHINA

zedg@sina.com

Abstract: - Fast parameter estimation of sinusoidal frequency modulation signal (SFM) in additive white Gaussian noise is considered. A technique based on Carson's rule is developed to estimate the frequency modulation index; the carrier frequency is calculated using the symmetrical property of side-frequency components; the instantaneous frequency is computed to get the modulation frequency. The Cramér-Rao lower bound (CRLB) of parameter estimation of SFM is also been derived. Monte Carlo simulations show that the parameter estimation accuracy is acceptable when the SNR is above $6dB$.

Key-Words: - Sinusoidal FM; Carson's Rule; Parameter estimation; Instantaneous frequency; CRLB.

1 Introduction

Frequency modulation (FM) is well known as the broadcast signal format for communication. In particular, the sinusoidal FM (SFM) signal is a kind of FM signal whose instantaneous frequency (IF) is modulated by sinusoidal signal. It is one of the most important signals with low probability of intercept in radar field, which has high range resolution, inhibits leakage and near field interference. Setlur modulated the micro-Doppler of radar signal for vibrations or rotations target or structures as SFM signal [1]. SFM signal has also been widely used in sonar, multipath communication channels, helicopter recognition and some other fields.

There are lists of algorithms for the estimation of FM signal. The most are based on time-frequency representations (TFRs) because of the non-stationarity of the SFM. Barbarossa combined the TFRs and pattern recognition methods for the analysis of nonlinear frequency modulation signals [2]; however, the computation complexity was heavy for electronic intelligence receiver. Barkat proposed a method to detect the presence of polynomial FM signal using the peak of polynomial Wigner-Ville distribution (WVD) [3], but it was noise sensitive and easily influenced by the cross terms. In these methods, the accuracy lies on the TFR image, and the computation is not acceptable for a real-time system. Besides, some other approaches have been discussed. Quatieri introduced an approach to the joint estimation of

sine-wave amplitude modulation and FM based on the transduction of frequency modulation into amplitude modulation by linear filters using the amplitude envelope of the outputs of two transduction filters of piecewise-linear spectral shape [4]. This approach is creative, but it needs design two filters and is not suitable for the real-time environment of radar intelligence. Lv treated SFM signal as a high order polynomial phase signal [5]. The algorithm derived the order and phase coefficients of SFM signal to estimate the carrier frequency, FM index, and modulating frequency. It is effective, but still need to be improved in order judgment.

Carson's rule is suitable for the estimation of bandwidth of the continuous FM (CFM) signal [7], and could definitely be brought to the special kind, namely, the SFM signal, which has a harmonic spectrum with harmonic amplitudes given by Bessel functions of the first kind. Carson's rule is a computation effective approach which just needs one fast Fourier transform (FFT). We analyze the spectrum of SFM signal, and use the Carson's rule to estimate the modulation index. Our aim is to find a fast and accuracy way to estimate the parameters of SFM signals.

The remainder of this paper is organized as follows. Section 2 gives the signal model and spectrum of SFM signal, and details Carson's rule. In Section 3, we analyze the characteristics of parameters of SFM signal, and give effective ways

to estimate them. In Section IV, we show the analysis for performance, and derive the cramer-rao lower bound (CRLB) of SFM signal under different signal to noise ratio (SNR). Moreover, the computation complexity is also discussed. Section 5 provides conclusions.

2 Signal Model and Carson's Rule

In this section, we will model the SFM signal firstly, and give its spectrum and Carson's rule.

2.1 Signal Model and Its Spectrum

Observations $s[0], s[1], \dots, s[N-1]$ of a SFM in additive noise are obtained according to the model

$$s[n] = A \cos(2\pi f_0 n + m_f \sin \omega_m n + \varphi_0) + w[n] \quad (1)$$

$$= A \cos \alpha_n + w[n], n = 0, 1, \dots, N-1$$

where

A amplitude;

f_0 carrier frequency;

m_f modulation index;

ω_m modulation angular frequency;

φ_0 initial phase;

$$\alpha_n = 2\pi f_0 n + m_f \sin \omega_m n + \varphi_0;$$

$w[0], w[1], \dots, w[N-1]$ independent Gaussian

random variables with zero mean and variance σ^2 .

The vector $[f_0 \ m_f \ \omega_m]^T$ is to be estimated.

Using Bessel function, $s[n]$ without noise could be rewrote as

$$s[n] = J_0(m_f) \cos(2\pi f_0 n) + \sum_{k=1}^{\infty} J_k(m_f) \{ \cos[(2\pi f_0 + k\omega_m)n] + (-1)^k \cos[(2\pi f_0 - k\omega_m)n] \} \quad (2)$$

where $J_k(m_f)$ are Bessel functions of the first kind

of order k .
$$J_k(m_f) = \sum_{m=0}^{\infty} \frac{(-1)^m (m_f/2)^{2m+k}}{m!(m+k)!},$$

$$J_{-k}(m_f) = (-1)^k J_k(m_f).$$

The Fourier transform of $s[n]$ is

$$S(\omega) = A \sum_{k=-\infty}^{\infty} J_k(m_f) \delta(\omega - 2\pi f_0 - k\omega_m) \quad (3)$$

Equation (3) demonstrates that the spectrum of a SFM signal is a discrete set of components, equally spaced at an interval of ω_m , namely, the modulation frequency. The spectrum is centered at, and

symmetrical about $2\pi f_0$. The amplitude of f_0 is $2\pi A J_0(m_f)$, and $2\pi A J_k(m_f)$ for $2\pi f_0 \pm \omega_m$.

Fig.1. shows the relation between $J_k(m_f)$ and m_f . It can be seen that $m_f = 1.4347$ is a turning point. When $m_f < 1.4347$, i.e., the signal is weakly modulated (WM), only the lowest order Bessel functions have significant amplitudes and the amplitude decreases as the increase of k . Signal energy is mostly concentrated in the vicinity of the carrier frequency. When $m_f > 1.4347$, i.e., the signal is highly modulated (HM), the spectrum becomes wideband with significant power occurring at considerable displacements from the carrier frequency. For certain values of the modulation index, $J_0(m_f)$ would be zero, i.e., the carrier has no energy.

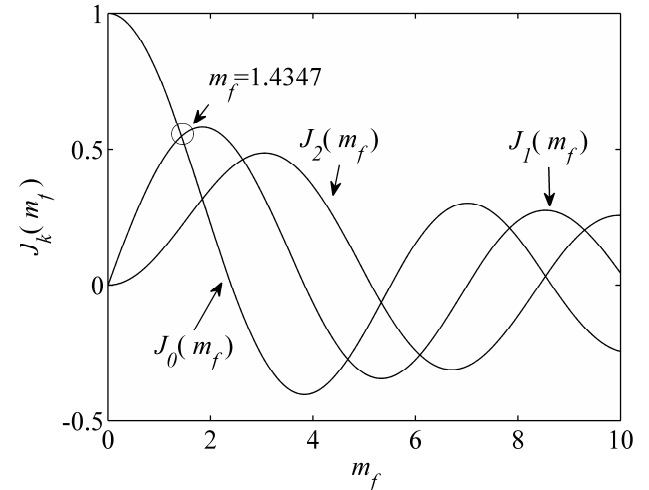


Fig. 1. The amplitude of $J_k(m_f)$ VS m_f .

2.2 Carson's Rule

SFM signal spectrum contains an infinite number of frequency components, in theory, infinitely wide band width. However, the amplitude of power spectra decreases with an increasing displacement in frequency from the carrier frequency, and $J_k(m_f)$ falls down when k grows. Therefore, we can take the appropriate k so the side-frequency components are small enough as to be ignored. In other words, SFM signal can be treated as finite bandwidth.

Theoretically any frequency modulation signal will have an infinite number of sidebands and hence an infinite bandwidth but in practice all significant sideband energy (98% or more) is concentrated within the bandwidth defined by Carson's rule. The rule can be derived from an examination of the spectra properties of CFM signal. It was shown that the spectral components of CFM signals consist of Bessel functions. Here, after enough simulations, we

think that the signal bandwidth should include sidebands whose power spectra are more than 10% of the power spectra of carrier frequency without modulation. Thus, $|J_k(m_f)| \geq 0.1$.

When $m_f \geq 1$, the power spectra of sidebands for $k > m_f + 1$ is less than 10% of the power spectra of carrier frequency without modulation, so we can set $k = m_f + 1$. There are $2k = 2(m_f + 1)$ sidebands, and the frequency interval between sidebands is ω_m , so the effective bandwidth of SFM signal is

$$B = 2(m_f + 1)\omega_m = 2(\Delta\omega + \omega_m) \quad (4)$$

where $\Delta\omega = m_f\omega_m$ is the frequency deviation.

Equation (4) is Carson's rule, which is used to estimate the bandwidth of frequency modulation signal.

When $m_f \ll 1$, (4) can be rewrote as

$$B \approx 2\omega_m \quad (5)$$

Therefore, when the modulation is too weak, the effective bandwidth is as twice as modulation frequency.

When $m_f \gg 1$, (4) can be rewrote as

$$B \approx 2\Delta\omega \quad (6)$$

Thus, when the modulation is too high, the effective bandwidth is as twice as frequency deviation.

3 Parameter Estimation

This section we will estimate the carrier frequency, modulation frequency and modulation index respectively.

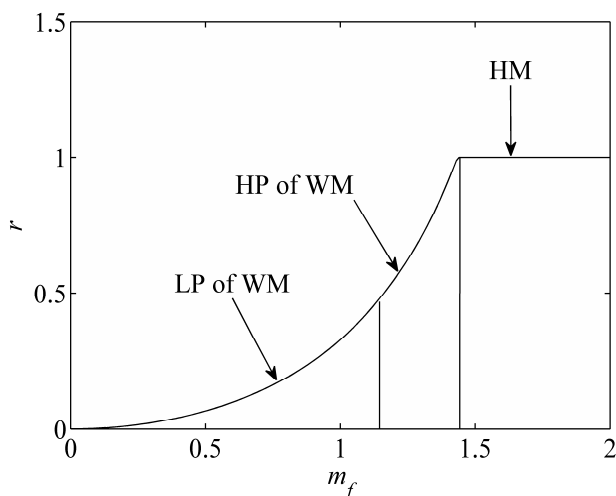


Fig. 2. The ratio r VS m_f theoretically.

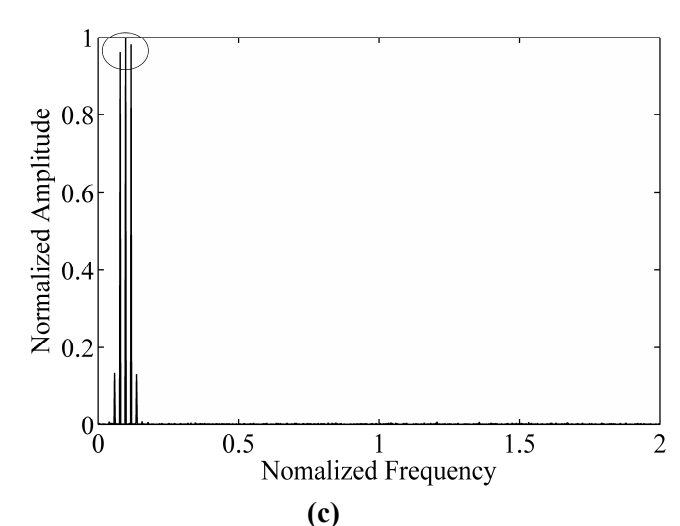
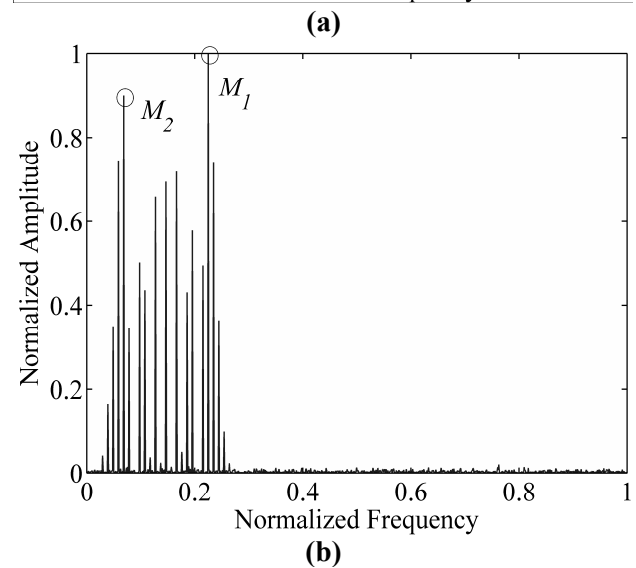
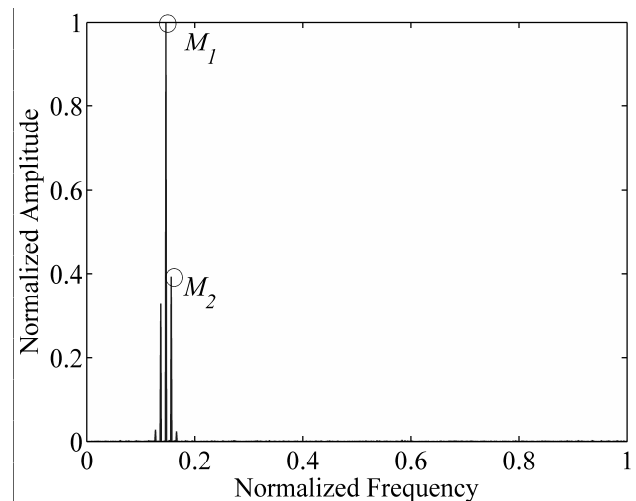


Fig. 3. The Spectrum of SFM with different modulation index when the SNR is 5dB.
(a) $m_f = 1$. (b) $m_f = 5$. (c) $m_f = 1.5$.

3.1 Carrier frequency

The power spectra of SFM signal is symmetrical about the carrier frequency, consequently, f_0 can be

estimated from the symmetric centre of scattered frequency components. The algorithm process is as follows:

- 1) Compute the power spectrum of $s[n]$;
- 2) Find the highest spectrum peak P_1 to determine its maximum value M_1 and the index ind_1 . Set the power spectrum whose index values in range $[ind_1 - 2 \ ind_1 + 2]$, then find the highest spectrum peak P_2 to determine its maximum value M_2 and the corresponding index ind_2 ;
- 3) Estimate the frequencies with respect to M_1 and M_2 , and denote them as \hat{f}_1 and \hat{f}_2 , respectively;
- 4) Calculate the ratio defined by $r = M_2 / M_1$. If $r \geq T_r$, the signal should be judged as WM signal, and the estimator for f_0 is

$$\hat{f}_0 = \hat{f}_1 \quad (7)$$

On the other hand, if $r < T_r$, the signal should be judged as HM signal, and the estimator is defined by

$$\hat{f}_0 = \frac{\hat{f}_1 + \hat{f}_2}{2} \quad (8)$$

- 5) Estimate the frequency using the algorithm in [8].

r is determined by $[J_1(m_f) / J_0(m_f)]^2$ when $J_1(m_f) \geq J_0(m_f)$, and its value keeps 1 when $J_1(m_f) < J_0(m_f)$ in theory. T_r is the threshold to choose the sub-estimator, which is important for the performance of the estimation. Here, we set $T_r = 0.5$ after enough simulations. If $r \leq 0.5$, there is only one obvious peak, as shown in area of low part of WM signal (LP of WM) in Fig.2 and Fig. 3(a), and we will locate f_0 accurately. If $r > 0.5$, there are two higher peaks obvious at least, which are related to HM or the area in high part of WM signal (HP of WM) in Fig.2 and Fig. 3(b). If there are three peaks whose energies are almost the same, as shown in Fig. 3(c), we need some modification which would be detailed in 3.2.

3.2 Modulation Frequency

The IF of SFM is

$$\omega_{SFM}[n] = 2\pi f_0 + m_f \omega_m \cos \omega_m n \quad (9)$$

The Fourier transform (FT) of $\omega_{SFM}[n]$ is

$$S(\omega) = \delta(\omega) + 0.5m_f \omega_m \delta(\omega - \omega_m) + 0.5m_f \omega_m \delta(\omega + \omega_m) \quad (10)$$

Filter out the DC component $\delta(\omega)$ in (11), and we will get the estimator for f_m :

$$\hat{\omega}_m = \arg \left\{ \max_{\omega \neq 0} |S(\omega)| \right\} \quad (11)$$

In order to improve the accuracy, we use [8] to estimate ω_m .

The estimator needs compute the IF, and the steps of the sub-algorithm are

- 1) Calculate the Hilbert transform of $s[n]$ using FFT and inverse FFT (IFFT), and denote the analytic signal as

$$z[n] = s[n] + jH(s[n]) \quad (12)$$

- 2) Estimate the instantaneous phase (IP) $\varphi[n]$:

$$\varphi[n] = \arctan \left\{ \frac{H(s[n])}{s[n]} \right\} \quad (13)$$

The phase $\varphi[n]$ has periodic ambiguity, and the algorithm for unwrapping the ambiguity is detailed in [9]. The final phase is $\hat{\varphi}[n]$.

- 3) Compute the linear fitting $\hat{L}[n]$ of $\hat{\varphi}[n]$, and let

$$\varphi_l[n] = \hat{\varphi}[n] - \hat{L}[n] \quad (14)$$

- 4) Filter $\varphi_l[n]$ by low pass filter (LPF) to eliminate the high frequency noise.
- 5) Compute the backward difference of $\varphi_l[n]$ as $\varphi_{lb}[n]$. The IF should be

$$\hat{\omega}_{SFM}[n] = \varphi_{lb}[n] f_s + \hat{L}[n] \quad (15)$$

Here, we use least square algorithm to fit $\hat{\varphi}[n]$ lineally. Its slope and intercept, namely S and I of $\hat{L}(n)$ are

$$\begin{cases} S = \frac{b_1 A_1 - b_2 N}{A_1^2 - A_2 N} \\ I = \frac{b_1 - S A_1}{N} \end{cases} \quad (16)$$

where $t[n] = [-\frac{N}{2}, -\frac{N}{2} - 1, \dots, \frac{N}{2} - 1]$, $A_1 = \sum_{n=0}^{N-1} t[n]$,

$$A_2 = \sum_{n=0}^{N-1} |t[n]|^2, \quad b_1 = \sum_{n=0}^{N-1} \hat{\varphi}[n] \quad \text{and} \quad b_2 = \sum_{n=0}^{N-1} t[n] \hat{\varphi}[n].$$

Hamming or Hanning window is considered for the LPF, and the cutoff frequency is designed as the last decline point after the highest frequency. The order M of window should be range from 30 to 60. Further explanations are given as follows. Take a SFM signal with $A=1$, $m_f=10$, $\omega_m=0.02\pi$, $\varphi_0=\pi/4$ and the sampling frequency $f_s=1\text{Hz}$ when the SNR is 5dB as an example. The noised signal is shown in Fig. 4(a) with SNR=5dB. The discrete-time IP is computed by (13) and be unwrapped to get $\hat{\varphi}[n]$ and its linear fitting $\hat{L}[n]$, as shown in Fig. 4(b). The backward difference is applied to estimate the IF, as shown in Fig. 4(c).

The spectrum of IF computed by FFT is shown in Fig. 4(d). As we can see, there is a sharp peak followed by a rapid decline, separating the signal and the high frequency noise. We can set the cutoff frequency as the last decline point after the highest frequency. From Fig. 4(d), the cutoff frequency should be 0.02559Hz. The output of the filter is shown in Fig. 4(e).

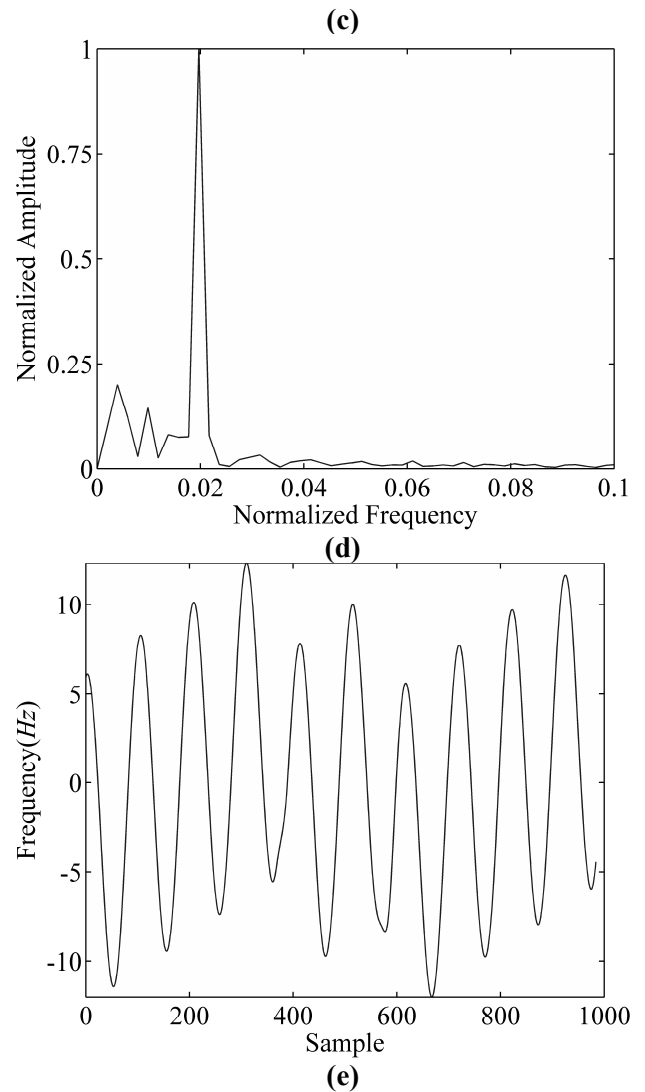
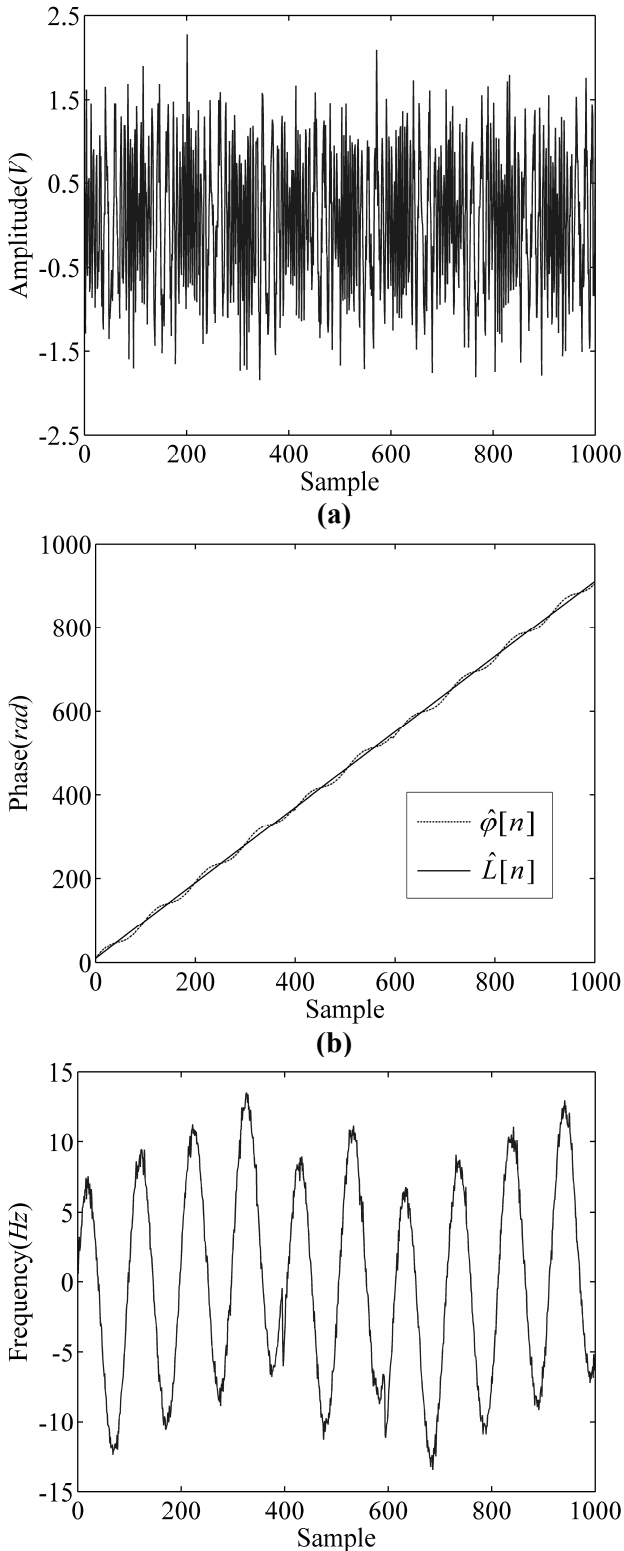


Fig. 4. An example to compute instantaneous frequency. (a) Noised signal when SNR=5dB. (b) Instantaneous phase and its linear fitting. (c) Instantaneous frequency with high frequency noise. (d) Spectrum of instantaneous frequency. NA stands for normalized amplitude. (e) Filtered instantaneous frequency.

As mentioned in 3.1, there would be some modification to fix the problem of location in the HP of WM and the LP of HM situation, i.e., when m_f lies in HP of WM, r may be greater than 0.01, and will be treated as HM. Therefore, we need a patch to fix the problem. After giving the IF, we could estimate the carrier frequency again after 3.1. If the outputs are almost the same, we will confirm the result in 3.1. While, if the two outputs are different a lot, we will add the following steps to 3.1.

- 1) If $r \leq 0.5$, confirm the result in 3.1, otherwise go to Step 2;
- 2) Compute the mean of the IF and denote it as \hat{f}'_0 . If $|\hat{f}'_0 - \hat{f}_0| \leq 0.002\text{Hz}$ (sampling frequency

is 1Hz), confirm the result in 3.1, otherwise go to Step 3;

- 3) Find the third highest spectrum peak P_3 to determine its maximum value M_3 and the corresponding index ind_3 ;
- 4) Compute the centre frequencies \hat{f}_{M_1} , \hat{f}_{M_2} and \hat{f}_{M_3} between ind_1 and ind_2 , ind_1 and ind_3 , ind_2 and ind_3 , respectively;
- 5) The selected output should be

$$\hat{f}_0 = \hat{f}_{M_q} \left\| \hat{f}_{M_q} - \hat{f}'_0 \right\| \leq \left| \hat{f}_{M_i} - \hat{f}'_0 \right|, i \in \{1, 2, 3\} \quad (17)$$
- 6) Estimate the frequency as [7].

3.3 Modulation Index

We should estimate the effective bandwidth before finding modulation index according (4). The amplitudes of side-frequencies are modulated by Bessel functions, and we need to use adaptive threshold to estimate the effective bandwidth of both weakly highly modulated signals. The flow is given by

- 1) Find the threshold $T_{MI} = cM_1$;
- 2) Estimate the effective bandwidth \hat{B} by comparing the power spectrum with T_{MI} .
- 3) The estimator of m_f is given by

$$\hat{m}_f = \frac{\hat{B}}{2\hat{\omega}_m} - 1 \quad (18)$$

The threshold c is different for highly and weakly modulated signals. When the signal is weakly modulated, the carrier frequency is the energy centre, and the energy of side-frequencies is comparatively low. Therefore, c should be a small value, but if c is too small to contain the noise level, there would be some mistakes. After enough simulations, it shows that $c = 0.01$ is an acceptable threshold. When SFM is highly modulated, the energy is distributed among side-frequencies, c values greatly. Similarly, if c is too great, there would be some mistakes, missing some energy of signal, and the estimated \hat{B} would be greater than the true value. c should be 0.09 after simulations. Another question is that how we determine the modulation index before its estimation. From 3.1 and 3.2, we can know that the modification can distinguish whether the signal is highly modulated.

In short, the flow of the algorithm is shown in Fig. 5.

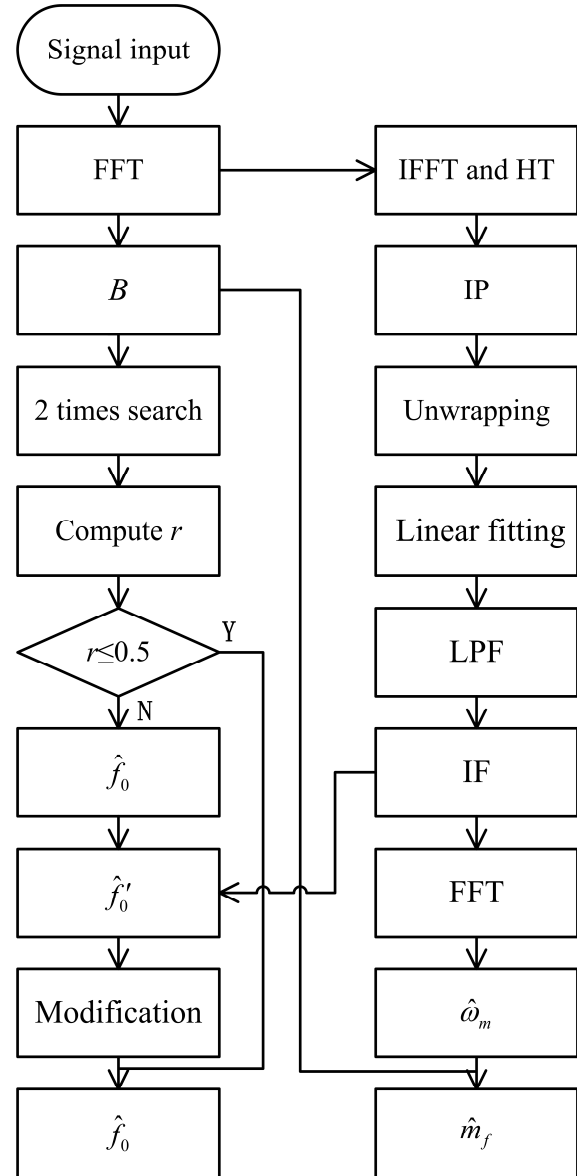


Fig. 5. Flow of the algorithm.

4 Performance Analysis

We will derive the CRLB of parameters of SFM signal at first, and show the simulation results under the conditions of weakly and highly modulation. Finally, the computation complexity will be discussed.

4.1 The CRLB of SFM Signal

Generalizing to vector signal parameter estimation in the presence of WGN, we have [9]

$$[\mathbf{I}(\boldsymbol{\theta})]_{ij} = \frac{1}{\sigma^2} \sum_{n=0}^{N-1} \frac{\partial s[n; \boldsymbol{\theta}]}{\partial \theta_i} \frac{\partial s[n; \boldsymbol{\theta}]}{\partial \theta_j} \quad (19)$$

as the elements of the Fisher information matrix.

Here, $s[n; \boldsymbol{\theta}] = s[n]$ and $\boldsymbol{\theta} = [A \ f_0 \ m_f \ \omega_m \ \varphi_0]^T$.

The derivatives are easily found as

$$\frac{\partial s[n; \boldsymbol{\theta}]}{\partial \boldsymbol{\theta}_1} = \frac{\partial s[n; \boldsymbol{\theta}]}{\partial A} = \cos \alpha_n \quad (20)$$

$$\frac{\partial s[n; \boldsymbol{\theta}]}{\partial \boldsymbol{\theta}_2} = \frac{\partial s[n; \boldsymbol{\theta}]}{\partial f_0} = -2\pi A n \sin \alpha_n \quad (21)$$

$$\frac{\partial s[n; \boldsymbol{\theta}]}{\partial \boldsymbol{\theta}_3} = \frac{\partial s[n; \boldsymbol{\theta}]}{\partial m_f} = -A \sin(\omega_m n) \sin \alpha_n \quad (22)$$

$$\frac{\partial s[n; \boldsymbol{\theta}]}{\partial \boldsymbol{\theta}_4} = \frac{\partial s[n; \boldsymbol{\theta}]}{\partial \omega_m} = -A m_f n \cos(\omega_m n) \sin \alpha_n \quad (23)$$

$$\frac{\partial s[n; \boldsymbol{\theta}]}{\partial \boldsymbol{\theta}_5} = \frac{\partial s[n; \boldsymbol{\theta}]}{\partial \varphi} = -A \sin \alpha_n \quad (24)$$

In evaluating the CRLB it is assumed that ω_m , $2\pi f_0 + m_f \omega_m \cos \omega_m n$, $2\pi f_0 + m_f \omega_m \cos \omega_m n \pm \omega_m / 2$ and $2\pi f_0 + m_f \omega_m \cos \omega_m n \pm \omega_m$ are not near 0, $\pi/2$ or π , which allows us to make certain simplifications based on approximations:

$$\begin{aligned} \sum_{n=1}^N \cos 2\alpha_n \approx 0, \quad \sum_{n=1}^N \sin 2\alpha_n \approx 0, \quad \sum_{n=1}^N n \sin 2\alpha_n \approx 0, \\ \sum_{n=1}^N n^2 \cos \omega_m n \approx 0, \quad \sum_{n=1}^N n \cos 2\alpha_n \approx 0, \quad \sum_{n=1}^N n^2 \cos 2\alpha_n \approx 0, \\ \sum_{n=1}^N \sin(2\alpha_n \pm \omega_m n) \approx 0, \quad \sum_{n=1}^N \cos(2\alpha_n \pm \omega_m n) \approx 0, \\ \sum_{n=1}^N n \sin(2\alpha_n \pm \omega_m n) \approx 0, \quad \sum_{n=1}^N n \cos(2\alpha_n \pm \omega_m n) \approx 0, \\ \sum_{n=1}^N n^2 \sin(2\alpha_n \pm \omega_m n) \approx 0, \\ \sum_{n=1}^N n^2 \cos(2\alpha_n \pm \omega_m n) \approx 0, \quad \sum_{n=1}^N \sin(2\alpha_n \pm 2\omega_m n) \approx 0, \\ \sum_{n=1}^N \cos(2\alpha_n \pm 2\omega_m n) \approx 0, \quad \sum_{n=1}^N n \sin(2\alpha_n \pm 2\omega_m n) \approx 0, \\ \sum_{n=1}^N n \cos(2\alpha_n \pm 2\omega_m n) \approx 0, \\ \sum_{n=1}^N n^2 \sin(2\alpha_n \pm 2\omega_m n) \approx 0 \quad \text{and} \\ \sum_{n=1}^N n^2 \cos(2\alpha_n \pm 2\omega_m n) \approx 0. \end{aligned}$$

Using these approximations, we have

$$\begin{aligned} [\mathbf{I}(\boldsymbol{\theta})]_{11} &= \frac{1}{\sigma^2} \sum_{n=0}^{N-1} \cos^2 \alpha_n \\ &= \frac{1}{\sigma^2} \sum_{n=0}^{N-1} \left(\frac{1}{2} + \frac{1}{2} \cos 2\alpha_n \right) \approx \frac{N}{2\sigma^2} \end{aligned} \quad (25)$$

$$[\mathbf{I}(\boldsymbol{\theta})]_{12} = -\frac{\pi A}{\sigma^2} \sum_{n=0}^{N-1} n \sin 2\alpha_n \approx 0 \quad (26)$$

$$[\mathbf{I}(\boldsymbol{\theta})]_{13} = -\frac{A}{2\sigma^2} \sum_{n=0}^{N-1} \sin(\omega_m n) \sin 2\alpha_n \approx 0 \quad (27)$$

$$[\mathbf{I}(\boldsymbol{\theta})]_{14} = -\frac{A m_f}{2\sigma^2} \sum_{n=0}^{N-1} n \cos(\omega_m n) \sin 2\alpha_n \approx 0 \quad (28)$$

$$[\mathbf{I}(\boldsymbol{\theta})]_{15} = -\frac{A}{2\sigma^2} \sum_{n=0}^{N-1} \sin 2\alpha_n \approx 0 \quad (29)$$

$$\begin{aligned} [\mathbf{I}(\boldsymbol{\theta})]_{22} &= \frac{1}{\sigma^2} \sum_{n=0}^{N-1} A^2 (2\pi n)^2 \sin^2 \alpha_n \\ &= \frac{(2\pi A)^2}{\sigma^2} \sum_{n=0}^{N-1} n^2 \left(\frac{1}{2} - \frac{1}{2} \cos 2\alpha_n \right) \\ &\approx \frac{2\pi^2 A^2}{\sigma^2} \sum_{n=0}^{N-1} n^2 \end{aligned} \quad (30)$$

$$\begin{aligned} [\mathbf{I}(\boldsymbol{\theta})]_{23} &= \frac{1}{\sigma^2} \sum_{n=0}^{N-1} 2\pi A^2 n \sin(\omega_m n) \sin^2 \alpha_n \\ &= \frac{2\pi A^2}{\sigma^2} \sum_{n=0}^{N-1} n \sin(\omega_m n) \left(\frac{1}{2} - \frac{1}{2} \cos 2\alpha_n \right) \approx 0 \end{aligned} \quad (31)$$

$$\begin{aligned} [\mathbf{I}(\boldsymbol{\theta})]_{24} &= \frac{1}{\sigma^2} \sum_{n=0}^{N-1} 2\pi A^2 n^2 m_f \cos(\omega_m n) \\ &\cdot \sin^2 \alpha_n = \frac{2\pi A^2 m_f}{\sigma^2} \sum_{n=0}^{N-1} n^2 \cos(\omega_m n) \\ &\cdot \left(\frac{1}{2} - \frac{1}{2} \cos 2\alpha_n \right) \approx 0 \end{aligned} \quad (32)$$

$$\begin{aligned} [\mathbf{I}(\boldsymbol{\theta})]_{25} &= \frac{1}{\sigma^2} \sum_{n=0}^{N-1} 2\pi A^2 n \sin^2 \alpha_n \\ &= \frac{2\pi A^2}{\sigma^2} \sum_{n=0}^{N-1} n \left(\frac{1}{2} - \frac{1}{2} \cos 2\alpha_n \right) \approx \frac{\pi A^2}{\sigma^2} \sum_{n=0}^{N-1} n \end{aligned} \quad (33)$$

$$\begin{aligned} [\mathbf{I}(\boldsymbol{\theta})]_{33} &= \frac{1}{\sigma^2} \sum_{n=0}^{N-1} A^2 \sin^2(\omega_m n) \sin^2 \alpha_n \\ &= \frac{A^2}{\sigma^2} \sum_{n=0}^{N-1} \left(\frac{1}{2} - \frac{1}{2} \cos(2\omega_m n) \right) \\ &\cdot \left(\frac{1}{2} - \frac{1}{2} \cos 2\alpha_n \right) \approx \frac{N A^2}{4\sigma^2} \end{aligned} \quad (34)$$

$$\begin{aligned} [\mathbf{I}(\boldsymbol{\theta})]_{34} &= \frac{1}{2\sigma^2} \sum_{n=0}^{N-1} A^2 m_f n \sin(2\omega_m n) \\ &\cdot \sin^2 \alpha_n = \frac{A^2 m_f}{2\sigma^2} \sum_{n=0}^{N-1} n \sin(2\omega_m n) \\ &\cdot \left(\frac{1}{2} - \frac{1}{2} \cos 2\alpha_n \right) \approx 0 \end{aligned} \quad (35)$$

$$\begin{aligned}
 [\mathbf{I}(\boldsymbol{\theta})]_{35} &= \frac{1}{\sigma^2} \sum_{n=0}^{N-1} A^2 \sin(\omega_m n) \sin^2 \alpha_n \\
 &= \frac{A^2}{\sigma^2} \sum_{n=0}^{N-1} \sin(\omega_m n) \left(\frac{1}{2} - \frac{1}{2} \cos(2\alpha_n) \right) \approx 0
 \end{aligned} \tag{36}$$

$$\begin{aligned}
 [\mathbf{I}(\boldsymbol{\theta})]_{44} &= \frac{1}{\sigma^2} \sum_{n=0}^{N-1} (A m_f)^2 n^2 \sin^2 \alpha_n \cos^2(\omega_m n) \\
 &= \frac{A^2 m_f^2}{\sigma^2} \sum_{n=0}^{N-1} n^2 \left(\frac{1}{2} - \frac{1}{2} \cos 2\alpha_n \right) \\
 &\cdot \left(\frac{1}{2} + \frac{1}{2} \cos(2\omega_m n) \right) \approx \frac{A^2 m_f^2}{4\sigma^2} \sum_{n=0}^{N-1} n^2
 \end{aligned} \tag{37}$$

$$\begin{aligned}
 [\mathbf{I}(\boldsymbol{\theta})]_{45} &= \frac{1}{\sigma^2} \sum_{n=0}^{N-1} A^2 m_f n \cos(\omega_m n) \sin^2 \alpha_n \\
 &= \frac{A^2 m_f}{\sigma^2} \sum_{n=0}^{N-1} n \cos(\omega_m n) \left(\frac{1}{2} - \frac{1}{2} \cos 2\alpha_n \right) \approx 0
 \end{aligned} \tag{38}$$

$$\begin{aligned}
 [\mathbf{I}(\boldsymbol{\theta})]_{55} &= \frac{1}{\sigma^2} \sum_{n=0}^{N-1} A^2 \sin^2 \alpha_n \\
 &= \frac{A^2}{\sigma^2} \sum_{n=0}^{N-1} \left(\frac{1}{2} - \frac{1}{2} \cos 2\alpha_n \right) \approx \frac{NA^2}{2\sigma^2}
 \end{aligned} \tag{39}$$

The Fisher information matrix has the symmetry property, i.e., $[\mathbf{I}(\boldsymbol{\theta})]_{ij} = [\mathbf{I}(\boldsymbol{\theta})]_{ji}$, so we have got the whole matrix. We have upon inversion

$$\begin{cases} \text{var}(\hat{f}_0) = \frac{3}{\pi^2 \eta N(N^2 - 1)} \\ \text{var}(\hat{m}_f) = \frac{2}{\eta N} \\ \text{var}(\hat{\omega}_m) = \frac{12}{\eta N(N-1)(2N-1)m_f^2} \end{cases} \tag{40}$$

where $\eta = A^2 / (2\sigma^2)$ is the SNR. The CRLBs for $\hat{\omega}_m$, \hat{f}_0 and \hat{m}_f decrease as the SNR increases and that the bound decrease as $1/N^3$, $1/N^3$ and $1/N$ respectively, making them quite sensitive to data record length. The bound for $\hat{\omega}_m$ is inversely proportional to m_f .

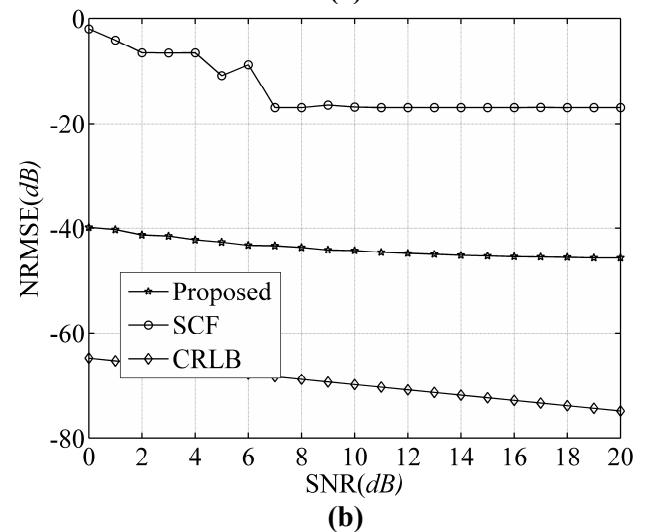
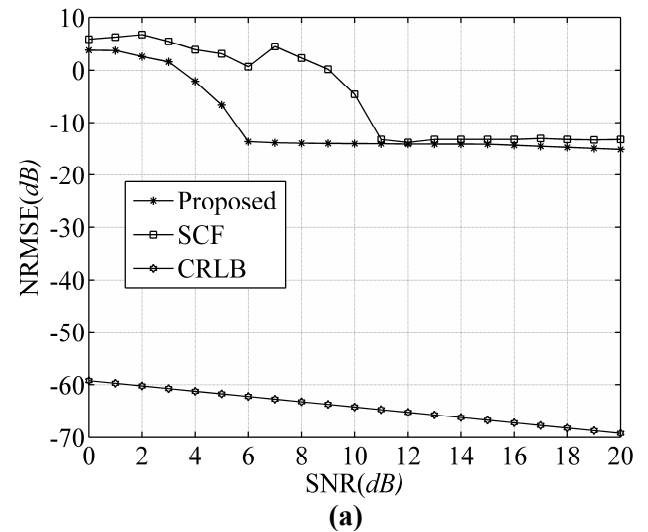
4.2 Weakly Modulated Signal

In simulations,

$$\begin{aligned}
 A &= 1; \\
 f_0 &= 0.05\text{Hz}; \\
 m_f &= 1; \\
 \omega_m &= 0.02\pi; \\
 \varphi &= \pi / 4.
 \end{aligned}$$

The sampling frequency is 1Hz. The number of sampling points is 1024. SNR ranges from 0 to 20. 500 times Monte-Carlo runs in each SNR. We compare the proposed algorithm with spectral correlation function (SCF) which is suitable for WM signal. Fig. 6 shows the estimation accuracy of the proposed method, the algorithm based on SCF and the CRLB. The NRMSE stands for normalized root mean square error.

When $SNR \geq 6\text{dB}$, this accuracy of modulation frequency estimation of the proposed method is about 20dB higher than the SCF. When $SNR \geq 11\text{dB}$, the both methods almost have the same performance, and the proposed method has slightly higher accuracy. Both of them are far away more than 50dB from the CRLB. For the estimation of carrier frequency, the accuracy of proposed method is more than 26dB higher than the SCF, and is looser than the CRLB about 25dB. The accuracy of modulation index of SCF is about 4dB less than the way of Carson's rule.



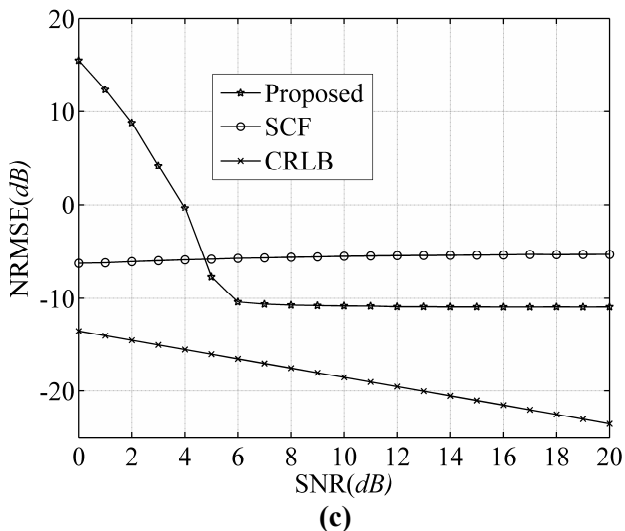


Fig. 6. The estimation accuracy of each parameter for weakly modulated signal. (a) ω_m . (b) f_0 . (c) m_f .

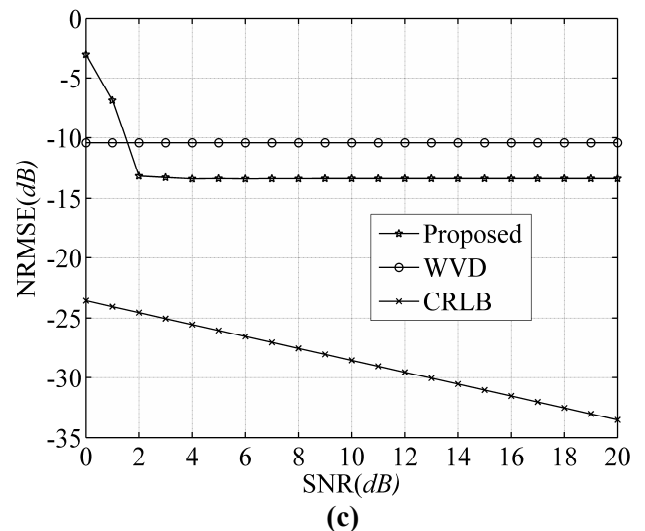
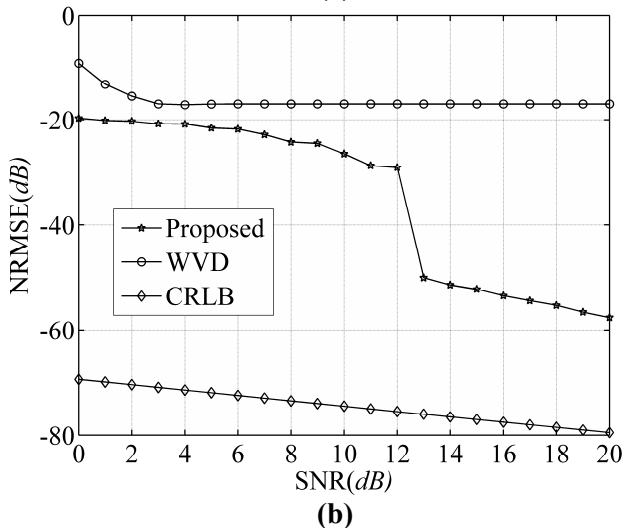
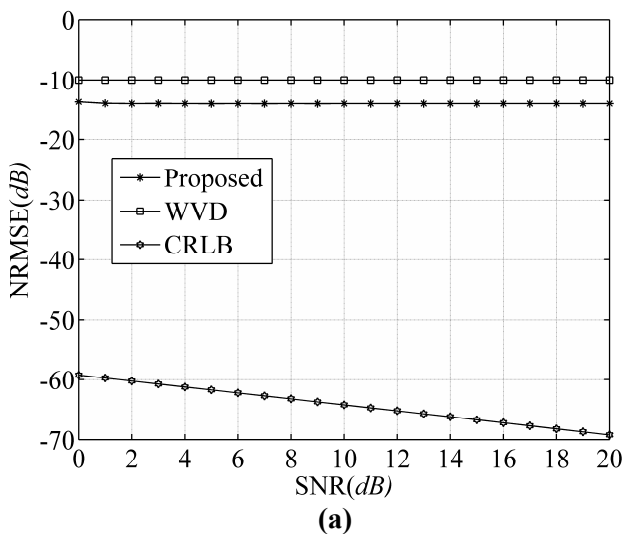


Fig. 7. The estimation accuracy of each parameter for highly modulated signal. (a) ω_m . (b) f_0 . (c) m_f .

4.3 Highly Modulated Signal



In simulations,

$$\begin{aligned}
 A &= 1; \\
 f_0 &= 0.15\text{Hz}; \\
 m_f &= 10; \\
 \omega_m &= 0.02\pi; \\
 \varphi &= \pi/4.
 \end{aligned}$$

We compare the proposed algorithm with Wigner-Ville distribution (WVD) which is suitable for HM signal. Fig. 7 shows the results. The accuracy of modulation frequency estimation of the proposed method is about 4dB higher than the algorithm in [11] in the considered SNRs. Both of them are far away from the CRLB more than 50dB. For the estimation of carrier frequency, the accuracy of proposed method is more than 33dB higher than the SCF when $SNR \geq 13dB$, and 4dB higher when $SNR \geq 6dB$. The proposed method is looser than the CRLB about 26dB when $SNR \geq 13dB$, and 50dB when $SNR \geq 6dB$. The accuracy of modulation index of SCF is about 3dB less than the way of Carson's rule.

When the signal is weakly modulated, the main component of spectrum is carrier frequency; therefore, it is easy to be located. The accuracy of carrier estimation is higher than the highly modulated one. In Fig. 6(c), the modulation index is small when the signal is weakly modulated, so the energy of side-frequency ω_m in (9) is also small, making the anti-noise capability poor. When $SNR \geq 6dB$, the algorithm converges. When the signal is highly modulated, the energy of carrier frequency is less than the one of side-frequency, and the energy differences among side-frequencies are

less the same. The carrier frequency algorithm accuracy decreased as shown in Fig. 7(b). The modulation index in Fig. 7(c) is relatively large, improving the anti-noise capability; as a result, the method will converges when $SNR \geq 2dB$.

The proposed method is based on the symmetric property of SFM signal to estimate the carrier frequency, making it only suitable for single signal. Carson's rule is particular for the continuous FM signal to estimate the effective bandwidth approximately, and its accuracy is not high. With the decrease of SNR, the carrier frequency estimation accuracy declines; the same time, the noise in IP will affects the IF estimation, leading to decreasing in modulation frequency and modulation index estimation accuracy.

4.4 Computation Complexity

Table 1. Computation complexity

| Par. | Function | Detail | Computation |
|------------|------------------------|--------------------|---|
| - | Hilbert | FFT and IFFT | $2M \log_2 N$ CMs |
| f_0 | PSD iterations | Square DFT | N CMs and 3 TSs $3N$ CMs |
| | IP | TE | $63N$ CMs |
| | LF | (16) | $6N-2$ CMs |
| ω_m | LPF | M -order | $2MN-N$ CMs |
| | FT of IF iterations | 1 FFT DFT | $M \log_2 N$ CMs $3N$ CMs |
| m_f | B | 1 search | 1 TS |
| all | - | - | About $3M \log_2 N + 75N + 2MN$ CMs+4TS |

The proposed method is based on the computation of FFTs, with some logical judge and search. The details of computation complexity are shown in Table 1. The complex multiplication (CM) and time of search (TS) are shown. TE stands for Taylor expansion; Par. is the abbreviation of parameter.

As we can see, there are 3 FFTs (IFFT) in total, and the times of multiplication are about $100N$ when M is about 30. The computation complexity is acceptable for hardware implementation.

5 Conclusion

In order to reduce the computation complexity of the existing algorithms for the parameters estimation

of sinusoidal frequency modulation signal, a fast method based on Carson's rule is presented in this paper. The carrier frequency was estimated by the symmetric property of the side-frequency, and was modified by the instantaneous frequency. The modulation frequency was computed by instantaneous phase dealt by linear fitting and low pass filter. Modulation index was derived from Carson's rule. When SNR is greater than $6dB$, all the sub-algorithms work well and are robust for weakly and highly modulated signals. The whole computation complexity is controlled at an acceptable level for real-time system. The further work will focus on the fast method for multi-component signals.

References:

- [1] P. Setlur, M. Amin, Thayaparan, T. T, "Micro-Doppler signal estimation for vibrating and rotating targets," *Proc. 8th Int. Symposium on signal processing and its application*, 2005, pp. 639 - 642.
- [2] S. Barbarossa, O. Lemoine, "Analysis of nonlinear FM signals by pattern recognition of their time-frequency representation," *IEEE Signal Processing Letters*, Vol.3, No.4, 1996, pp. 112-115.
- [3] B. Barkat, B. Boashash, "Instantaneous frequency estimation of polynomial FM signals using the peak of PWVD: statistical performance in the presence of additive Gaussian noise," *IEEE Trans. on SP*, Vol.47, No.9, 1999, pp. 2480-2490.
- [4] T. F. Quatieri, T. E. Hanna, G. C. O'Leary, "AM-FM separation using auditory-motivated filters," *IEEE Trans. on Speech and Audio Processing*, Vol.5, No.5, 1997, pp. 465-480.
- [5] Y. Lv, J. Zhu, B. Tang, "SFM signal parameter estimation based on discrete polynomial-phase transform," *IET Int. Radar Conf.*, 2009, pp.376.
- [6] J. H. Yin, Y. Hua, W. L. Yang, et al, "On the use of a linear data model for parameter estimation of sinusoidal FM signals," *Int. Conf. on Communications, Circuits and Systems*, 2009, pp. 387 - 390.
- [7] R. G. Wiley, *ELINT: The interception and analysis of radar signals*, Artech House, 2006.
- [8] E. Aboutanios, B. Mulgrew, "Iterative frequency estimation by interpolation on Fourier coefficients," *IEEE Trans. on SP*, Vol. 53, No. 4, 2005, pp. 1237-1242.
- [9] M. Sun and R. J. Sclabassi, "Discrete-time instantaneous frequency and its computation," *IEEE Trans. on SP*, Vol. 41, NO. 5, 1993, pp. 1867-1880.

- [10] S. M. Kay. *Fundamentals of statistical signal processing, Vol I: Estimation theory*, Prentice Hall PTR, 1993.
- [11] V. Katkovnik and L. Stankovic. "Instantaneous Frequency Estimation Using the Wigner Distribution with Varying and Data-Driven Window Length," *IEEE Trans. on SP*, Vol. 46, No. 9, 1998, pp. 2315-2325.